Accurate modeling of impinging jet heat transfer

By M. Behnia, S. Parneix AND P. Durbin

1. Motivation and objectives

In the last two decades, jet impingement heat transfer has received considerable attention because of its many applications for high heat flux cooling or heating. There are numerous papers dealing with this problem both numerically and experimentally. Some reviews have also appeared, amongst which some of the most recent are Jambunathan *et al.* (1992), Viskanta (1993), and Webb & Ma (1995).

There are a number of parameters which can affect the heat transfer rate in a jet impingement configuration. For instance, the jet-to-target distance not only affects the heat transfer rate, but also can have a significant effect on the local heat transfer coefficient distribution (Baughn & Shimizu, 1989). For the design and optimization of jet impingement cooling or heating systems, it is essential that the effect of these parameters of importance be characterized. In some of the previous studies, these effects have been addressed, and results of the experiments performed by different investigators have sometimes been contradictory due to the differences in the experimental conditions. In their review, Jambunathan *et al.* (1992) clearly pointed out this problem and noted that, for a better understanding of the jet impingement heat transfer process, the details of the flow, geometry, and turbulence conditions are required so that a comparison between different experimental data can be made.

Due to the difficulties in performing and comparing experiments, a numerical simulation of the problem would have been an ideal candidate for quantifying the effect of the parameters of interest. However, turbulent impinging jets have complex features due to entrainment, stagnation, and high streamline curvature. These features prove to be incompatible with most existing turbulence models, which are essentially developed and tested for flows parallel to a wall. For instance, Craft *et al.* (1993) have demonstrated some of the problems in these turbulence models, namely a substantial over-prediction of heat transfer in the stagnation region by the widely used $k-\varepsilon$ turbulence model. In fact, the complexity of this flow has led to it being chosen as an excellent and challenging test-case (see ERCOFTAC database at http://fluindigo.mech.surrey.ac.uk) for the validation of turbulence models. A number of investigators have gauged the success of their models based on this flow. However, turbulence modelers encounter numerous difficulties due to the fact that the details of the experimental data are often not known or that the flow conditions and geometry are not well posed.

For validation purposes, we chose the data sets obtained in a fully-developed impinging jet configuration (i.e. Baughn & Shimizu 1987, Baughn *et al.* 1989, Lytle & Webb 1995, Yan 1993 and Mesbah 1996). Some computations with the flat plate configuration (Fig. 1) at a single Reynolds number have been reported in the 1996

CTR Annual Research Briefs (Behnia *et al.* 1996). It has been shown that the *V2F* model successfully and economically predicted the rate of heat transfer. Subsequent simulations are presented in this report to determine the effects of important parameters such as jet-to-target distance, geometry, and Reynolds number, as well as jet confinement.

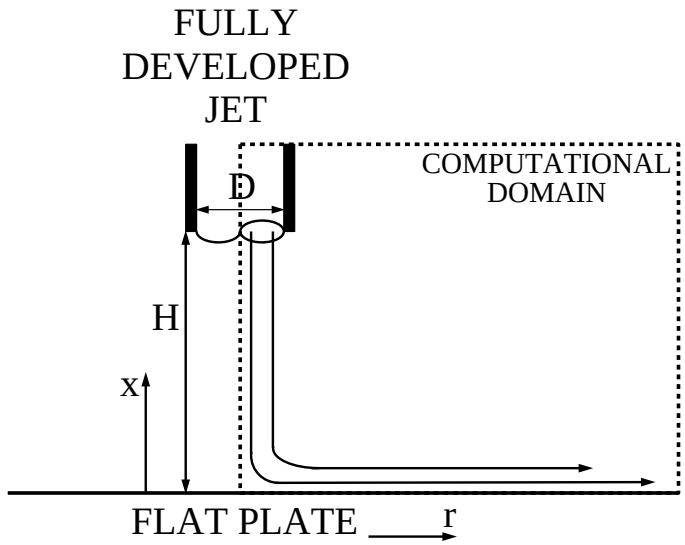

FIGURE 1. Configuration of the jet impinging on a flat plate.

2. Accomplishments

2.1 Background

2.1.1 Simulation techniques

Most predictions of jet impingement heat transfer in industry involve the use of standard or modified versions of the $k-\varepsilon$ turbulence model, available in all existing CFD packages. These models have usually been developed, calibrated, and validated using flows parallel to the wall. Physical phenomena involved in impinging flows on a solid surface are substantially different and have been considered as highly challenging test-cases for the validation of turbulence models. For example, simulations from Craft *et al.* (1993) of a non-confined impinging jet cooling a heated flat plate, using a $k-\varepsilon$ type model, showed dramatically poor results for wall heat transfer coefficients (e.g. more than 100% over-prediction in the stagnation region).

The *V2F* turbulence model, introduced by Durbin (1991, 1993b), could be thought of as a restriction of a full Second Moment Closure model developed subsequently (Durbin 1993a). It has the advantage of keeping an eddy viscosity, which avoids some computational stability problems encountered with Reynolds-stress closure models. It is a general geometry turbulence model, valid right up to the solid wall. It does not need wall functions, whose universality is increasingly being called into question, especially in impinging regions. The alternative is the introduction of damping functions, which are tuned to mimic the near-wall effects. But all these

models use a single-point approach that cannot represent the well-known, non-local effects of pressure-reflection that occur near solid boundaries. Moreover, these damping functions often involve an ill-defined normal distance to the wall, which cannot be used in complex configurations. They are also highly non-linear and sometimes introduce numerical stiffness.

The *V2F* model brings more physics in its body. First, it introduces a new velocity scale, $\overline{v^2}$, used for the evaluation of the turbulent viscosity, instead of k; $\overline{v^2}$ might be regarded in some cases as the velocity fluctuation normal to the streamlines. It is equivalent to the turbulent kinetic energy, k, far from any solid walls; in the near-wall region, it becomes the velocity fluctuation normal to the solid surface, irrespective of the orientation of the surface relative to the flow. Theoretically, k is unable to represent the damping of turbulent transport close to the wall, whereas normal velocity fluctuations provide the right scaling (Behnia *et al.* 1997). Following the full Reynolds stress analysis (Durbin 1993a), in order to model non-local characteristics of the near-wall turbulence and to avoid the use of two-point correlations, which are not viable for non-homogeneous turbulence, the *V2F* model uses an elliptic operator to compute a term analogous to the pressure-strain correlation. Ellipticity is introduced by a modified Helmholtz operator, which is amenable to numerical computations and which introduces wall effects by a linear equation, taking care of the transition between the near-wall region and regions far from solid boundaries. Finally, some physical constraints have been added in order to prevent non-realizability of the solution, especially in the stagnation region (Durbin 1996).

The temperature field is computed through a standard eddy diffusivity approximation. Concerning the turbulent Prandtl number, Pr_t, the Kays and Crawford formulation (1993) was chosen for all of the following computations, including those with $k-\varepsilon$, since it gave a more physical representation near the wall (Pr_t increases from 0.85 in the far-field to about 1.7 in the near wall-region) and yielded somewhat better agreement in the impingement region. Nevertheless, the improvement over using a constant value is of the order of 10% (Behnia *et al.* 1997), which cannot explain the 100% error of the $k-\varepsilon$ model. The flow and the turbulent fields have to be accurately resolved for obtaining good heat transfer predictions. The basis and equations of the complete *V2F* model can be found in Behnia *et al.* (1996).

All computations were performed with INS2D, a general geometry, finite difference code developed by Rogers and Kwak (1990). The spatial discretization of convective terms was via a third order, upwind biased scheme; diffusion terms were central differenced. Fine, non-uniform, orthogonal, cylindrical grids were used, with a high resolution near all solid boundaries. A mesh sensitivity was carried out by dividing each mesh by 2 in the axial and radial directions. This changed the impingement region Nusselt number by less than 1%; therefore, the present solutions are considered grid-independent.

The flow conditions at the nozzle exit may affect the computed flow field. Therefore, for validation purposes, we chose the case of a jet coming from a long pipe so that nozzle-exit conditions are fully turbulent and well defined. A fully-developed

turbulent pipe flow was first computed in a preliminary computation and then interpolated onto the grid to provide the inlet condition of the jet. The flow domain began approximately 2 pipe diameters upstream of the jet exit so that the pipe profiles may evolve in the nozzle as the flow approaches the nozzle outlet. It is noted that prescribing the inlet conditions upstream of singularities is also a requirement in other types of flows, e.g. the backward-facing step. Further, in the unconfined case, this allows the upper computational boundary to be a sufficient distance from the wall that it does not affect the flow near the impingement surface.

2.1.2 The impinging jet on a flat plate

Some computations of jet impingement heat transfer have been reported in the 1996 CTR Annual Research Briefs (Behnia *et al.* 1996). The main conclusions of that paper are summarized on Figs. 2a and 2b. Computational results are presented for the widely-used test-case of an unconfined impinging jet on a flat plat at $Re = 23,000$ and for a nozzle-to-plate distance of 6 jet diameters. One can see that the experimental results are fairly well reproduced by the *V2F* model; in fact, the simulation falls into the range of available experimental data sets, represented by the gray zone of Fig. 2a. In comparison, the $k-\varepsilon$ model strongly over-predicts the heat transfer rates in the stagnation region (by about 100%). This over-estimation extends up to $2-3$ jet diameters away from the stagnation point, although the flow has already been parallel to the surface at this location. This indicates that the quantitative misbehavior spreads up in the region surrounding the impinging area and may influence the whole distribution of heat transfer, even qualitatively.

The excellent *V2F* results have been confirmed by studying the influence of the nozzle-to-target spacing, H/D, on the stagnation Nusselt number. Experimental data of Baughn & Shimizu (1989), Baughn *et al.* (1991), Yan (1993), and Lytle & Webb (1995) are plotted on the same graph, and a line of best fit has been evaluated for comparison purposes. A set of 15 simulations has been performed for each model and plotted against the available experimental data sets (Fig. 2b). The *V2F* model is in very good agreement with the experimental curve of best fit, with an optimal stagnation heat transfer rate at $H/D = 6-7$. Note that this optimal value has already been reported in numerous experimental studies (e.g. Martin 1977, Baughn & Shimizu 1989, Webb & Ma 1995). The quantitative over-prediction of the $k-\varepsilon$ model is present for all nozzle-to-plate spacings. If one wants to use this model for design purposes, the efficiency of the cooling system would be over-estimated; however, more dramatically, its optimization would also fail completely. For instance, the $k-\varepsilon$ model predicts 2 optimal nozzle-to-plate distances of 2.5 and 5 diameters, in total disagreement with the experiments.

2.2 Influence of Reynolds number

Turbulence models are sometimes fitted for a given test-case, at a given Reynolds number and might give much worse results when flow conditions are changed. Thus, it is essential to check the range of validity of the results obtained by the *V2F* model in the 1996 report for $Re = 23,000$. The dependence on the nozzle-to-plate distance has already been shown to be well captured by the model.

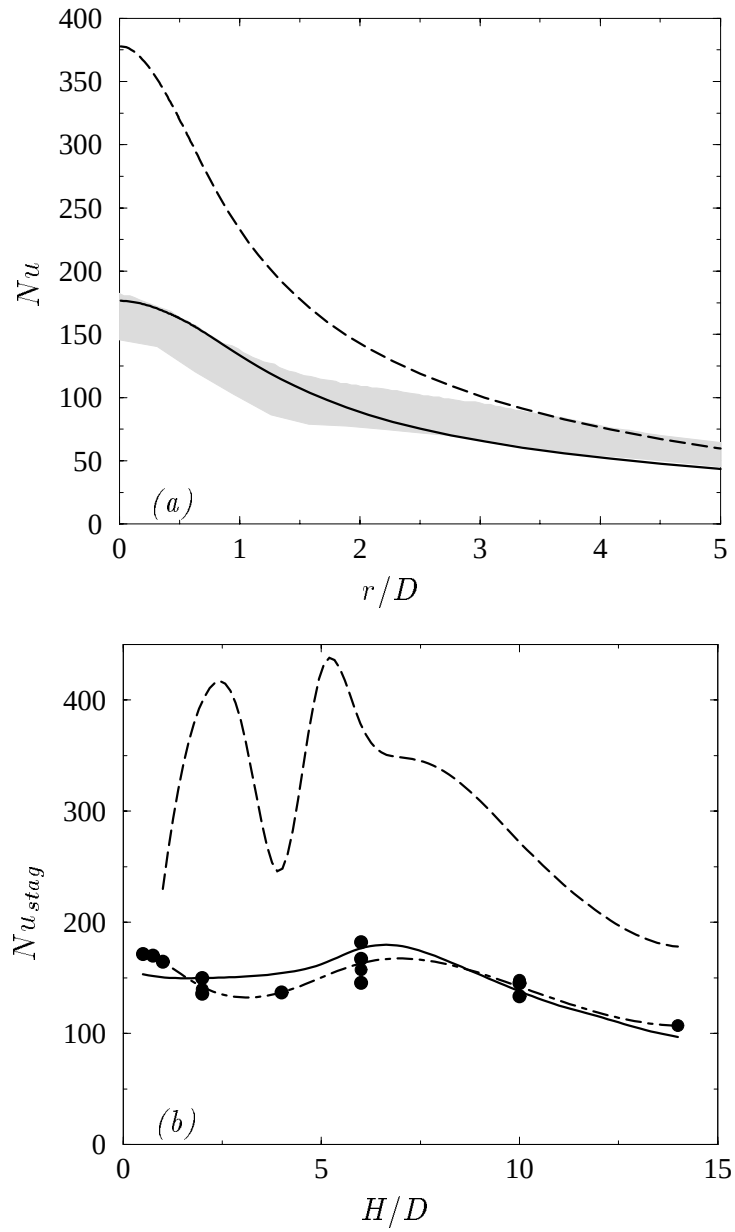

FIGURE 2. Impinging jet on a flat plate, $Re = 23,000$ (a) Local distribution of wall heat transfer for $H/D = 6$, (b) Dependence of stagnation wall heat transfer on H/D, ——— *V2F*, - - - - : $k - \varepsilon$, gray zone and • : experiments, —·— : line of best fit of experimental data.

The evolution of the local Nusselt number on the flat plate with increasing Reynolds number is presented for $H/D = 2$ (Fig. 3). Comparisons are with Yan's (1993) experimental data. One can observe an augmentation with Re of the relative height of the secondary peak in the Nu distribution. The model is qualitatively consistent with the experiment. As for the lower Reynolds number, this peak is less pronounced in the computations, but its location is very well predicted (around $r/D = 2$). Recall that a 20% scatter existed in the experimental data at

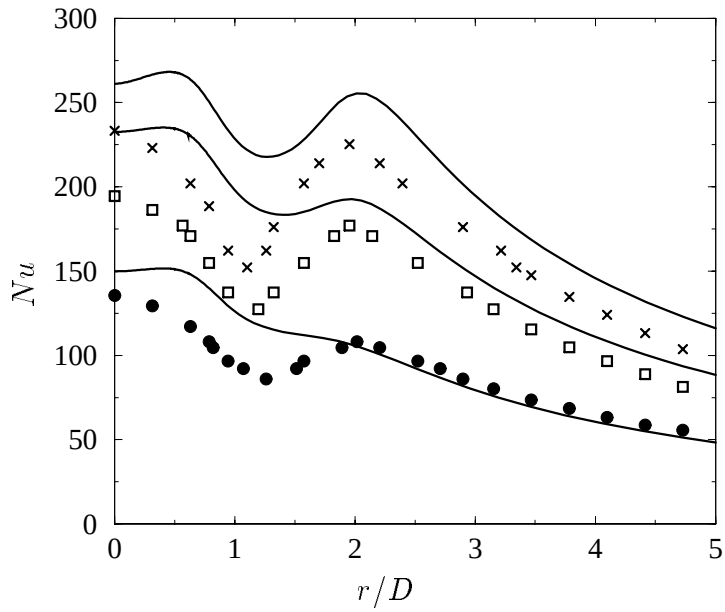

FIGURE 3. Influence of Reynolds number on the local distribution of wall heat transfer at $H/D = 2$, ——— : *V2F*, symbols: experiments (• : $Re = 23,000$, □ : $Re = 50,000$, × : $Re = 70,000$).

$Re = 23,000$ and that Yan's data were systematically close to the lowest quantitative bound on the whole set of available data. In light of this, the *V2F* results may be considered quite good.

Figure 4 presents the stagnation Nusselt number obtained for different flow rates at $H/D = 6$. The experimental data from Lytle & Webb (1995) and Yan (1993) are plotted on the same graph and a line of best fit has been evaluated for comparison purposes. One can see that the dependence on Reynolds number, predicted by the *V2F* model, is in excellent agreement with the experimental data. In particular, the quasi-laminar correlation $Nu_{stag} \propto Re^{0.5}$ has been obtained accurately. Of course, the Re number is high enough to assure a turbulent regime; for instance, Viskanta (1993) noted that heat transfer rates are $1.4 - 2.2$ times as high as the laminar rates. Moreover, a *V2F* correlation, showing the Nusselt number evaluated at 6 jet diameters away from the stagnation point, for different jet-to-plate distances, has been added to Fig. 4. Here, a dependence on $Re^{0.77}$ is predicted by the *V2F* model, in good agreement with previous experiments, which have established a dependence on $Re^{0.7-0.85}$ (see Jambunathan *et al.* 1992, Viskanta 1993).

2.3 Influence of the impinging surface's geometry

Very little experimental and computational work has been done on impinging flows in geometries other than flat plates. The objective of the work in this section has been to accurately compute the flow and thermal fields in an axisymmetric isothermal fully developed jet perpendicular to a heated pedestal mounted on a flat plate (Fig. 5). The geometry resembles that of an electronic component. Recently, Mesbah (1996) has measured the local heat transfer coefficient in this configuration.

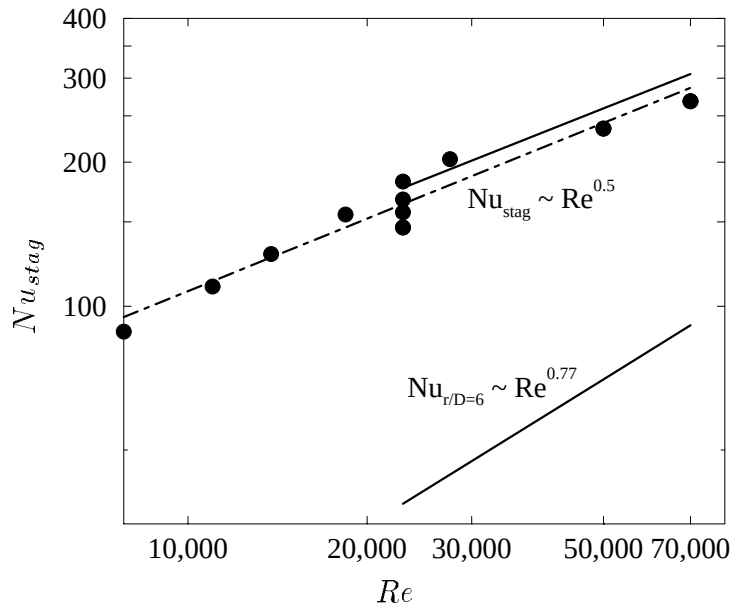

FIGURE 4. Influence of Reynolds number on the wall heat transfer coefficient for $H/D = 6$, at the stagnation point ($r/d = 0$) and at $r/D = 6$, ——— : *V2F*, • : experiments ($r/D = 0$), —·— : line of best fit of the stagnation experimental data.

He used the preheated-wall transient technique in conjunction with surfaces coated by thermochromic liquid crystals. For comparison purposes, we adopted the same geometry. In addition, computations were also performed using the widely used standard $k - \varepsilon$ turbulence model.

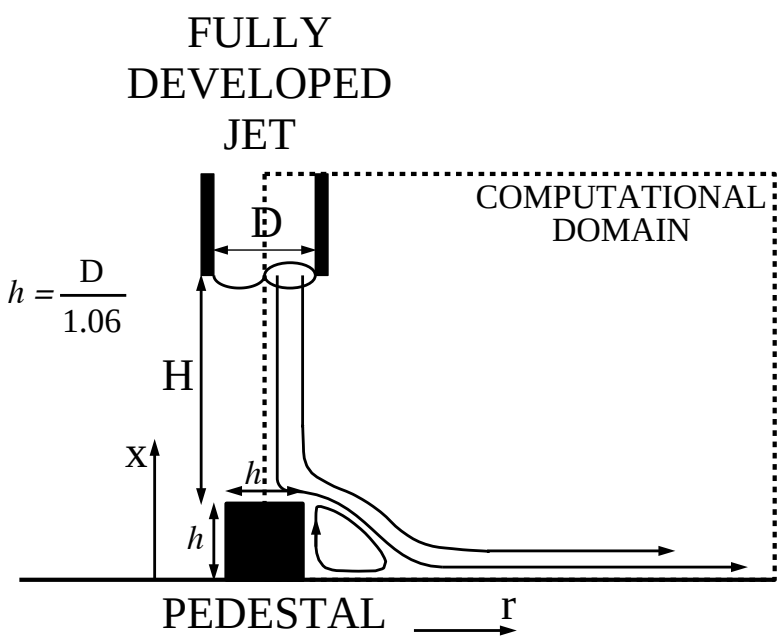

FIGURE 5. Configuration of the jet impinging on a wall-mounted pedestal.

Contours of Stokes streamlines are shown in Fig.6 for $H/D = 6$. Only a qualitative analysis will be done since no flow measurements are available. The flow, parallel to the jet axis at the nozzle exit, develops into a free jet before decelerating in the axial direction on top of the pedestal. Then, it turns sharply and starts to form a radial wall jet along the upper surface of the pedestal. At the corner, the flow separates and re-attaches downstream on the plate. This creates a recirculation which has a significant effect on the wall heat transfer. This bubble is much shorter than that found downstream of a backward-facing step (recirculation lengths between 5 and 8 times the step height); the rather short length is due to the strong influence of the outer region of the impinging jet and to the choice of an axisymmetric configuration. After reattachment, the flow develops into a wall jet along the plate. The ambient fluid outside the jet is entrained into the core with a developing shear layer separating the core and the ambient fluid. This entrainment is shown by the curvature of the streamlines outside the pipe towards the symmetry axis and leads to a small recirculation zone in the vicinity of the exit pipe-wall. This feature and the presence of a secondary recirculation near the bottom of the pedestal indicate a sufficient grid resolution around the exit of the nozzle and next to the pedestal.

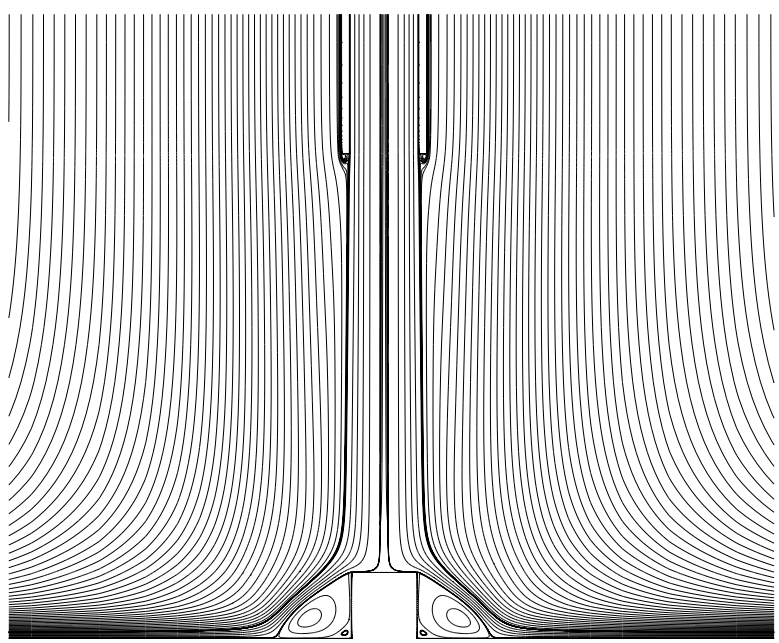

FIGURE 6. Streamlines for $H/D = 6$ computed with the *V2F* model.

We evaluated the temperature distribution for $H/D = 6$ using an isothermal boundary condition along the upper surface of the pedestal and downstream of it, on the plate (Fig. 7). The local wall heat transfer coefficient has a local minimum on the stagnation line on top of the pedestal. The Nu number is nearly constant in the vicinity of the stagnation point and then increases sharply as the corner is approached. The value of stagnation Nusselt number is similar to that of a jet

impinging on a flat plate. However, the local Nusselt number distribution is radically different from the flat plate configuration since, in that case, the stagnation Nusselt number is a local maximum. Hence, the flat plate results may not be suitable for complex geometries that can be found in some industrial applications. Figure 7 shows that the *V2F* model reproduces this behavior in the vicinity of the symmetry line, whereas the $k-\varepsilon$ predictions show a local maximum and a sharp decrease of Nu. Quantitatively, $k-\varepsilon$ predictions over-estimate the wall heat transfer above the whole pedestal upper surface by more than 150%. This over-prediction is believed to be due to the over-prediction of turbulent kinetic energy in that region (note the dark gray zone in Fig. 8). The use of $\overline{v^2}$ as the velocity scale instead of k for computing ν_t is essential here (Behnia *et al.* 1997), and therefore the *V2F* computations are much more realistic with only 5 to 15% of over-prediction. It is recalled that, for the impinging jet on a flat plate, the set of available experiments shows a 20% data scatter (Behnia *et al.* 1996). Moreover, Mesbah (1996) used the transient technique which gave results in the lower band of this experimental data set in the stagnation region. With this in mind, one can say that the *V2F* predictions are excellent.

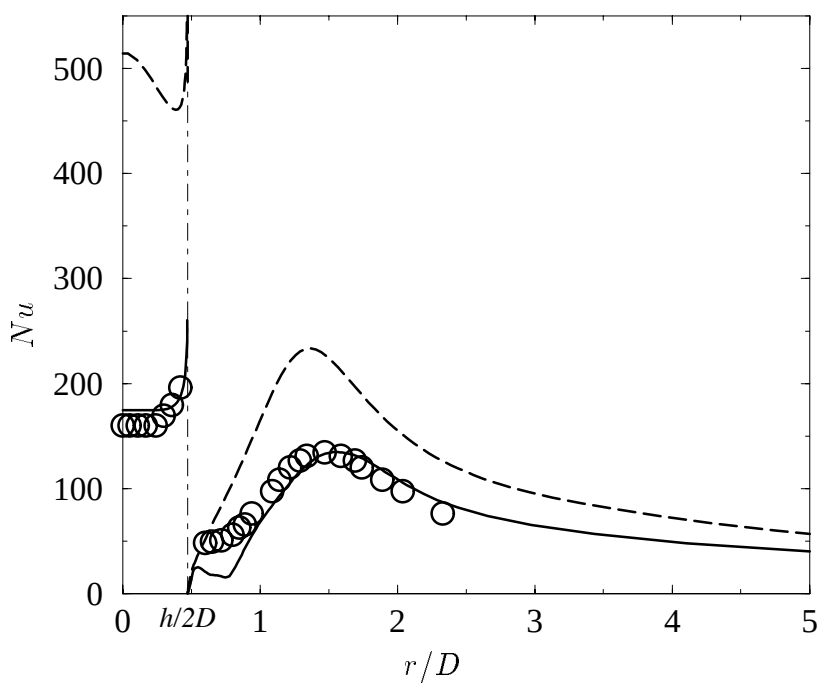

FIGURE 7. Local wall heat transfer coefficient for $H/D = 6$ and $Re = 23,000$ on top of the pedestal (left of —·—) and downstream of it on the flat plate (right of —·—), ——— : *V2F*, - - - - : $k-\varepsilon$, ○ : Mesbah's experiment (1996).

Along the plate, a local maximum wall heat transfer point is created in the reattachment region, about one diameter downstream of pedestal and slightly upstream of the reattachment point, as might be expected from the backward-facing step results (see Vogel & Eaton 1985). The *V2F* model predicts both the location and

magnitude of this peak accurately; $k-\varepsilon$ predictions still show almost 100% over-prediction, which may be more due to the diffusion of the dramatic heat transfer over-prediction on top of the pedestal rather than to an over-prediction of turbulence production in the reattachment area. The angle of impingement is much smaller (between 30° and 40°) in the reattachment region than around the symmetry axis. Finally, the *V2F* simulations show a plateau with a secondary peak at the foot of the pedestal. This phenomenon is believed to be due to the existence of a secondary recirculation. The plateau is present in the experiment, but without any secondary maximum. We suspect that in the experiment, longitudinal heat transfer in the solid near the corners of the pedestal occurs. Also, the longer times required for measurements in this region make the underlying assumption of the measurement technique questionable (Mesbah, 1996). Therefore, a constant temperature or constant heat flux assumption would not be accurate any more, which may explain the discrepancy.

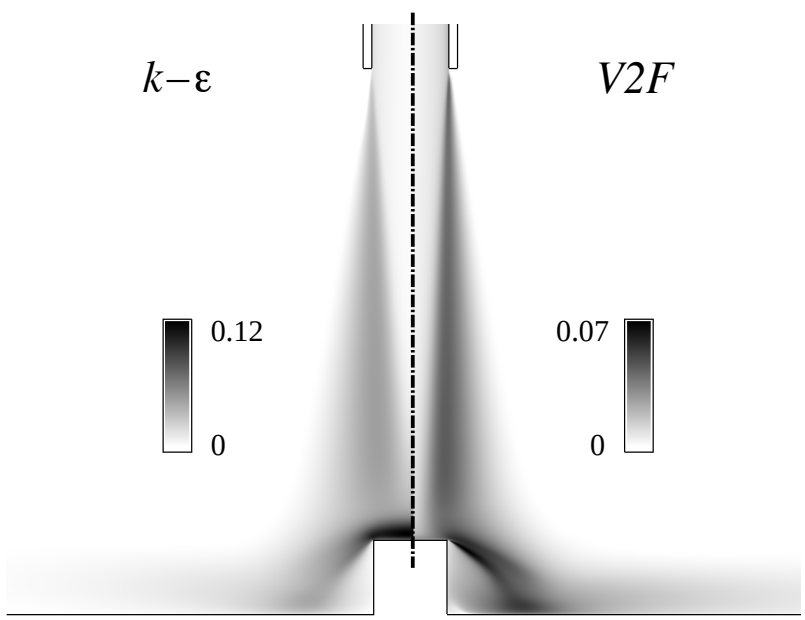

FIGURE 8. Contours of turbulent kinetic energy for $H/D = 6$. Overprediction of turbulent kinetic energy is reflected in the darkest gray area on top of the pedestal.

Simulations have been carried out for a fixed Reynolds number ($Re = 23,000$) and a wide range of aspect ratios ($1 \leq H/D \leq 8$) to determine the dependence on H/D of the stagnation Nusselt number on top of the pedestal and the local maximum Nusselt number on the plate. The behavior of Nusselt number variation with the jet-to-pedestal distance needs to be known for the design and optimization of impingement cooling or heating systems. Figures 9a and 9b show the corresponding values computed with both the *V2F* and $k-\varepsilon$ models. The *V2F* computations show very good agreement with Mesbah's experiment. As indicated before, the transient technique yielded results in the lower band of the flat plate experimental data set, so the 5 to 15% over-prediction is remarkable. Moreover, it is noted that

this over-prediction is almost constant; the dependence of stagnation Nusselt number on H/D is very well reproduced. Note also that the *V2F* computations show the existence of a maximum of stagnation heat transfer in the range $6 < H/D < 7.5$. This cannot be compared to Mesbah's experiment, since $H/D = 6$ was the highest aspect ratio studied, but this is consistent with previous flat plate results (Martin 1977, Baughn & Shimizu 1989, Behnia *et al.* 1996). The $k-\varepsilon$ model fails to reproduce the experimental trends, not only quantitatively (150% of over-prediction) but also qualitatively, which is even more critical from a practical point of view. Regarding the maximum Nusselt number downstream of the pedestal along the plate, both models reproduce a constant decrease with H/D. The $k-\varepsilon$ computations yield almost 100% over-estimated values, whereas *V2F* simulations are very close to the experiment. The only disagreement is for $H/D = 4$ where the experimental maximum Nusselt number is higher than for $H/D = 1$ and 2. Perhaps more experimental data points should be obtained to assess this non-monotonic behavior.

2.4 Effect of confinement

All the previous computations have been performed for an unconfined geometry. However, industrial applications, especially in electronic cooling, require the impinging jet to be confined with a solid boundary at the level of the nozzle exit. Numerous experiments have been conducted in order to study the effect of confinement on jet impingement heat transfer. The aim was mainly to know whether the physics and correlations involved in unconfined geometries could be applied in a confined context. Obot *et al.* (1982) concluded there was a reduction in the average heat transfer rate from 5 to 10% when confinement was added. Again, comparisons are difficult to establish from different experiments when jet outlet profiles or experimental conditions are different. Moreover, to our knowledge, no experimental data are available for a fully-developed jet coming from a long pipe. Since *V2F* simulations gave satisfactory results in the unconfined geometry, we assume that the model is accurate enough to undertake a numerical comparison study.

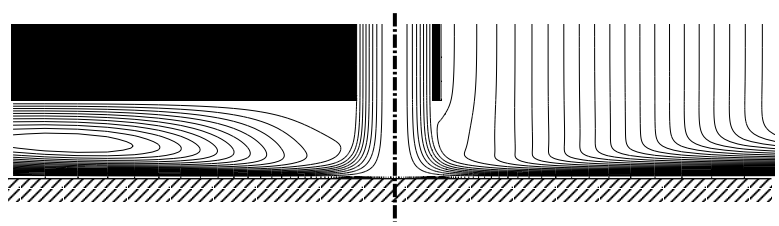

FIGURE 10. Streamlines for $H/D = 1$ and $Re = 23,000$ computed with the *V2F* model for the confined (left) and unconfined (right) configurations.

Several computations have been performed by adding a wall at the nozzle exit (Fig. 10). We varied the nozzle-to-plate distance, and the local heat transfer rates are compared to the results obtained with an unconfined geometry. Figure 11 shows the Nusselt number distribution for different H/D. One can see that, for a high enough jet-to-plate spacing, the confinement has no effect on the heat transfer rate. The presence of a top wall creates a recirculation (Fig. 10), but its influence

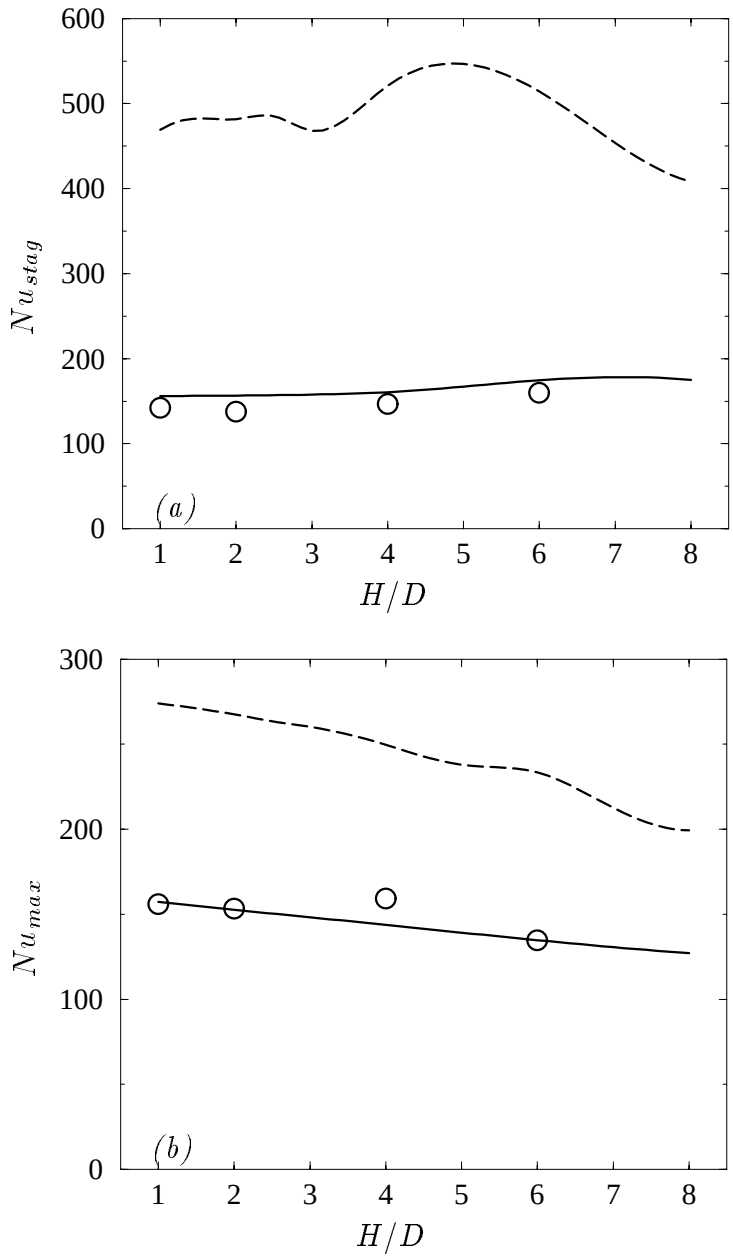

FIGURE 9. Impinging jet on a pedestal at $Re = 23,000$, influence of nozzle-to-plate distance on (a) the stagnation heat transfer coefficient on top of the pedestal and (b) the maximum heat transfer coefficient downstream of the pedestal along the plate, ——— : *V2F*, - - - - : $k - \varepsilon$, ○ : Mesbah's experiment (1996).

is rather small. Indeed, for $H/D > 1$, no significant difference in the wall heat transfer distribution has been observed. For $H/D < 0.5$, the Nusselt distributions start to diverge. As it has been found in experiments, the average heat transfer rate is slightly lower for the unconfined case. It can be explained by the fact that the top wall introduces a resistance to the flow; the entrainment of the external fluid by the jet is less important, decreasing the global efficiency of the impinging

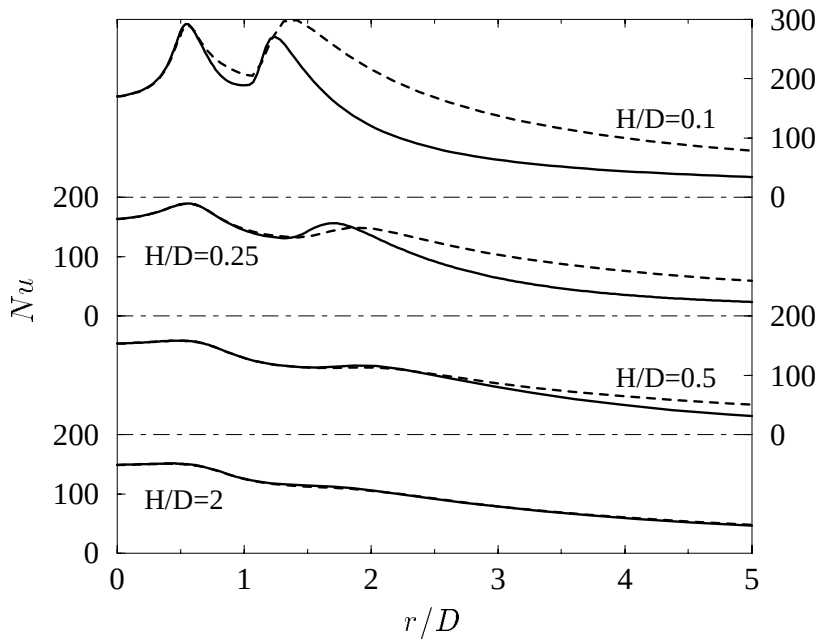

FIGURE 11. Local wall heat transfer, simulated by the *V2F* model, for the jet impinging on the flat plate at $Re = 23,000$ and different nozzle-to-plate distances ($H/D = 2$, 0.5, 0.25, and 0.1) ——— : confined, - - - - : unconfined.

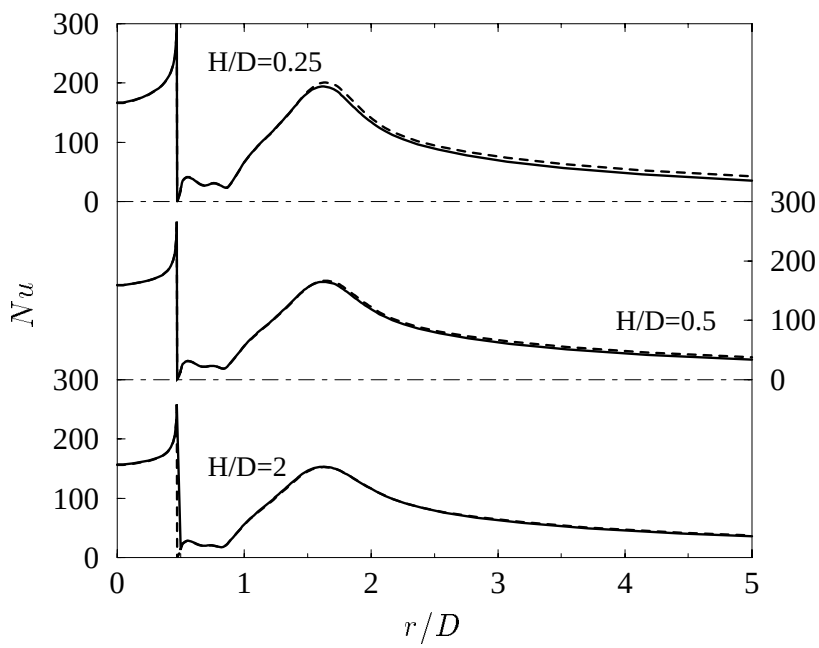

FIGURE 12. Local wall heat transfer, simulated by the *V2F* model, for the jet impinging on the pedestal at $Re = 23,000$ and different nozzle-to-plate distances ($H/D = 2$, 0.5, and 0.25) ——— : confined, - - - - : unconfined.

jet heat transfer. In the case of a smaller nozzle-to-plate distance (not shown here), the recirculation is more confined and active; it is located closer to the target plate and then has a stronger influence on the wall heat transfer coefficient. Nevertheless, even for a very low H/D (as low as 0.1), the stagnation heat transfer rates are not noticeably influenced by the presence of confinement. Up to a radial distance of 0.5 jet diameters away from the stagnation point, the Nu distributions stay unchanged whether the jet is confined or not. This is partially confirmed by Garimella & Rice (1995) who noted that, for $H/D > 2$, confinement had little effect on heat transfer at stagnation point. A primary peak is created at $r/D \simeq 0.5$ as H/D decreases. This peak corresponds to the acceleration of the local velocity, which occurs for $H/D < 0.25$. Its location is fixed, in good agreement with Colucci & Viskanta experiment (1996). A secondary peak is also created, but this time, its location is moving toward the axis of symmetry when the nozzle-to-plate distance is decreased. Again, such a behavior has been found to be in good qualitative agreement with Colucci & Viskanta experiment (1996). Similar computations have been performed for the case of the wall-mounted heated pedestal. One can see in Fig 12 that the influence of confinement is much less effective than for the flat plate configuration. Even for $H/D = 0.25$, heat transfer rates stay unchanged. First, the diameter of the pedestal is slightly smaller than the jet diameter. Thus, through the analysis of the previous results for the flat plate, no confinement effect was expected on top of the pedestal ($r/D < 0.5$). Downstream of it, on the plate, the top wall is then at a normalized distance of more than one jet diameter ($H/D + 1/1.06$); this distance is too high to expect any significant change in the heat transfer rate. Moreover, the recirculation, which strongly acts on the Nusselt distribution, is driven by the jet itself and is less subject to be affected by the confinement.

In conclusion, the confinement, present in most industrial applications, does not have a significant impact on the wall heat transfer coefficient unless the jet-to-target spacing is considerably reduced ($H/D < 0.25$). The average Nusselt number decreases with confinement, but the local heat transfer distribution in the stagnation region ($r/D < 0.5$) is not modified; unconfined impinging jet stagnation Nusselt number correlations can thus be used.

3. Future plans

The main aim of this research has been to assess the ability of computational fluid dynamics to accurately and economically predict the heat transfer rate in an impinging jet situation, strongly relevant to industrial applications, e.g. in electronic cooling. The computations carried out herein show that predictions by the normal-velocity relaxation model (*V2F* model) agree very well with the experiments. The influence of parameters of interest such as nozzle-to-plate distance, Reynolds number, geometry of the impingement surface, or confinement has been shown to be well captured. In comparison, the widely-used $k - \varepsilon$ model does not properly represent the flow features, highly over-predicts the rate of heat transfer, and yields physically unrealistic behavior.

It is planned to perform additional computations to cover a wider range of parameters (e.g. 3D configurations and a range of Prandtl numbers). In particular,

for electronic cooling applications, dielectric liquids in a confined jet geometry and multiple jets configurations need to be explored.

REFERENCES

BAUGHN, J., HECHANOVA, A. & YAN, X. 1991 An experimental study of entrainment effects on the heat transfer from a flat surface to a heated circular impinging jet. *J. Heat Transfer.* **113,** 1023-1025.

BAUGHN, J. & SHIMIZU, S. 1989 Heat transfer measurements from a surface with uniform heat flux and an impinging jet. *J. Heat Transfer.* **111,** 1096-1098.

BEHNIA, M., PARNEIX, S. & DURBIN, P., 1996 Simulation of jet impingement heat transfer with the $k - \varepsilon - \overline{v^2}$ model. *Annual Research Briefs,* Center for Turbulence Research, NASA Ames/Stanford Univ., 3-16.

BEHNIA, M., PARNEIX, S. & DURBIN, P., 1997 Accurate predictions of jet impingement heat transfer. *HTD-Vol. 343 National Heat Transfer Conference.* **5,** Book No H0190, 111-118.

COLUCCI, D. & VISKANTA, R. 1996 Effect of nozzle geometry on local convective heat transfer to a confined impinging air jet. *Experimental Thermal and Fluid Science.* **13,** 71-80.

CRAFT, T., GRAHAM, L. & LAUNDER, B. 1993 Impinging jet studies for turbulence model assessment–II. An examination of the performance of four turbulence models. *Int. J. Heat Mass Transfer.* **36**(10), 2685-2697.

DURBIN, P. 1991 Near-wall turbulence closure without damping functions. *Theoretical and Computational Fluid Dynamics.* **3**(1), 1-13.

DURBIN, P. 1993a A Reynolds-stress model for near-wall turbulence. *J. Fluid Mech.* **249,** 465-498.

DURBIN, P. 1993b Application of a near-wall turbulence model to boundary layers and heat transfer. *Int. J. Heat and Fluid Flow.* **14**(4), 316-323.

DURBIN, P. 1995 Separated flow computations with the $k - \varepsilon - \overline{v^2}$ model. *AIAA J.* **33**(4), 659-664.

DURBIN, P. 1996 On the $k - \varepsilon$ stagnation point anomaly. *Int. J. Heat and Fluid Flow.* **17,** 89-90.

GARIMELLA, S. & RICE, R. 1995 Confined and submerged liquid jet impingement heat transfer. *J. Heat Transfer.* **117,** 871-877.

JAMBUNATHAN, K., LAI, E., MOSS, M. & BUTTON, B. 1992 A review of heat transfer data for single circular jet impingement. *Int. J. Heat and Fluid Flow.* **13**(2), 106-115.

KAYS, W. M.& CRAWFORD, M. E. 1993 Convective heat and mass transfer. Third Edition, McGraw-Hill.

LYTLE, D. & WEBB, B. 1994 Air jet impingement heat transfer at low nozzle-plate spacings. *Int. J. Heat Mass Transfer.* **37,** 1687-1697.

MARTIN, H. 1977 Heat and mass transfer between impinging gas jets and solid surfaces. *Advances in Heat Transfer.* **13,** 1-60.

MESBAH, M. 1996 An experimental study of local heat transfer to an impinging jet on non-flat surfaces: a cylindrical pedestal and a hemispherically concave surface. *PhD Thesis,* University of California, Davis.

OBOT, N., MUJUMDAR, A. & DOUGLAS, W. 1982 Effect of semi-confinement on impinging heat transfer. *Proc. 7th Int. Heat Transfer Conf.* **3,** 395-400.

ROGERS, S. & KWAK, D. 1990 Upwind differencing scheme for the time-accurate incompressible Navier-Stokes equations. *AIAA J.* **28,** 253-262.

VISKANTA, R. 1993 Heat transfer to impinging isothermal gas and flame jets. *Exp. Thermal Fluid Sci.* **6,** 111-134.

VOGEL, J.C. & EATON, J.K. 1985 Combined heat transfer and fluid dynamic measurements downstream of a backward-facing step. *J. Heat Transfer.* **107,** 922-929.

WEBB, B. & MA, C.-F. 1995 Single-phase liquid jet impingement heat transfer. *Advances in heat transfer.* **26,** 105-217.

YAN, X. 1993 A preheated-wall transient method using liquid crystals for the measurement of heat transfer on external surfaces and in ducts. *PhD Thesis,* University of California, Davis.